Journal of Applied Mathematics and Computational Mechanics 2026, 25(3), 56-68
www.amcm.pcz.pl p-ISSN 2299-9965
DOI: 10.17512/jamcm.2026.3.04 e-ISSN 2353-0588

INFLUENCE OF SURFACE ROUGHNESS OF CIRCULAR STRESS CONCENTRATORS ON THE DISTRIBUTION OF STRENGTH PARAMETERS WITHIN STRUCTURAL ELEMENTS

***Petro Pukach*[1], *Andriy Havrylyak*[2], *Oleg Kuzin*[3], *Mykola Kuzin*[1, 4, *]**

[1] *Department of Computational Mathematics and Programming, Lviv Polytechnic National University
Lviv, Ukraine*
[2] *Department of Applied Mathematics, Lviv Polytechnic National University
Lviv, Ukraine*
[3] *Department of Applied Mechanics and Mechanical Engineering Technology
Ukrainian National Forestry University
Lviv, Ukraine*
[4] *Railway Transport Research Laboratory, Lviv Research Institute of Forensic Expertise
Lviv, Ukraine*
*petro.y.pukach@lpnu.ua, andriy.r.havrylyak@lpnu.ua, kuzinolegan@gmail.com
mykola.o.kuzin@lpnu.ua*

Received: 22 April 2026; Accepted: 29 July 2026

Abstract. A numerical analysis of strength parameters in structural elements containing circular stress concentrators is performed, taking into account the roughness of their internal surfaces. Based on continuum mechanics and mathematical modeling approaches, a problem formulation is proposed to assess the influence of stress concentrator roughness on the strength of the structure. The use of modern computational mechanics tools (namely, the FEniCS finite element analysis package and its Python implementation) makes it possible to determine the optimal surface roughness of the stress concentrator, which is found to lie in the range of $0.7\text{-}0.8\cdot 10^{-6}$ m. Under these conditions, the relative size of the region with enhanced strength increases, whereas further increases in roughness lead to significant weakening of the structural element.

MSC 2010: *74S05, 74P10, 74B05*
Keywords: *mathematical models, computational mechanics, stress concentrators, finite element method, surface roughness, optimization*

1. Introduction

One of the important features of modern mechanical engineering is the widespread use of components containing various stress concentrators of both physical and geometric origin.

[*] Corresponding author

During operation under service loads, such concentrators can significantly alter the stress-strain state of the material in local regions and affect the reliability of the entire structure [1].

The relevance of this problem, both from theoretical and applied perspectives, is reflected in numerous publications. Theoretical studies are mainly concerned with determining the influence of the morphology of geometric and physical stress concentrators on the stress state of components and their performance characteristics using analytical or numerical methods. Due to strong practical demand, the volume of publications in this area is steadily increasing. In this regard, it is worth noting the comprehensive works [2-5], which provide an overview of modern mathematical approaches for analyzing the influence of macrogeometric parameters of stress concentrators (their basic shape, orientation, and mutual arrangement) on strength and durability under given loading conditions.

Applied studies of stress concentrators are concerned with establishing relationships between manufacturing processes and the overall performance of components. In particular, studies [6-12] demonstrate the influence of fabrication processes of stress concentrators on residual stresses, the formation of damage and microcracks in the material, and changes in the roughness and microstructure of surface layers, which in turn determine the durability of components under specified operating conditions.

A characteristic feature of these works is their focus on analyzing changes in surface topology for each specific technological method of producing stress concentrators. This is explained by the engineering orientation and interdisciplinary nature of such studies, as they lie at the intersection of such scientific fields as fracture mechanics, continuum and damage mechanics, materials processing technology, and materials science. The complexity of accounting for variations in the surface parameters of stress concentrators within mathematical models using analytical relationships necessitates the use of computational mathematics tools and their implementation on high-performance computing systems. This creates significant challenges in solving such problems.

Overall, it can be stated that the issues related to identifying the influence of surface topology parameters and near-surface layers of stress concentrators on the reliability of components during operation remain open and insufficiently studied.

Without neglecting the role of physical factors governing the structural state of near-surface material layers around stress concentrators in shaping the operational characteristics of components, this study focuses on investigating the role of surface geometry in the distribution of strength parameters in local regions.

2. Problem formulation

The morphology of geometric stress concentrators can vary significantly [13-15]. In classical solid mechanics and engineering studies, they are predominantly modeled using smooth surfaces with a smoothness level of one or higher (e.g., circles, ellipses). This is due to the possibility of geometrically approximating the surfaces using well-known analytical relations, which are subsequently incorporated into the solution of the corresponding problems by means of methods based on holomorphic functions of a complex variable. Stress concentrators with more complex geometries, such as polygons, which are approximated by surfaces with zero smoothness, are considerably more difficult to analyze. In such cases, analytical relations become impractical, and numerical methods are therefore employed.

At the same time, each type of stress concentrator has specific effects on the formation of the stress-strain state in structural elements.

Circular stress concentrators form a stress state characterized by a one-dimensional directional change around the concentrator. Elliptical stress concentrators are more critical in terms of structural performance, as they lead to the formation of regions with high stress gradients in the vicinity of their tips. It is precisely in these regions that material weakening processes and microcrack propagation occur, as confirmed by both theoretical analyses and experimental data. Rectangular and polygonal stress concentrators act as sources of complex stress states, especially near their vertices. Depending on the vertex angle, the resulting stress state is characterized by high gradients and pronounced spatial non-uniformity, which significantly affects the mechanisms of material weakening in local regions of structural elements.

However, modeling the real geometry of stress concentrators solely by their macrogeometry is limited, as it ignores more complex surface features such as roughness. This roughness may arise as a result of controlled technological processes during the manufacturing of components.

To assess the influence of the surface geometry of stress concentrators, the following problem formulation is proposed.

Let a body (structural element) occupying a domain X in Euclidean space be given. The boundary of the domain is denoted by ∂X and represented as the following set:

$$\partial X = \partial X_1 \cup \partial X_2 \cup \partial X_3, \tag{1}$$

where ∂X_1 is the portion of the boundary where the loads are prescribed, ∂X_2 is the portion where displacements or boundary constraints are prescribed, ∂X_3 is the unloaded portion of the boundary.

To analyze the behavior of the continuum under external loading, a continuum model is employed that allows for both spatial variation of elastic properties and the distribution of damage [16]:

$$\vec{\nabla} \cdot \left(\frac{K(x)}{1-\omega(x)} \left(\vec{\nabla} \cdot \vec{u} \right) \hat{I} + \frac{2G(x)}{1-\omega(x)} \left(\vec{\nabla} \otimes \vec{u} - \frac{1}{3} \left(\vec{\nabla} \cdot \vec{u} \right) \hat{I} \right) \right) = 0, \tag{2}$$

where $\vec{u}$ is the displacement vector, $\hat{I}$ is the identity tensor, $\vec{\nabla}$ is the nabla differential operator, $K(x)$ is the bulk modulus, $G(x)$ is the shear modulus, $\omega(x)$ is the damage parameter, $\otimes$ denotes the dyadic product, $\cdot$ denotes the scalar product, $x \in X$.

In expression (2), damage is understood as a continuum measure of structural degradation, which can be described by a scalar function $\omega(x)$ [1, 13]. In this paper, it is assumed that $\omega(x)=0$, and the elastic properties of the material are constants.

It is further assumed that the domain under consideration contains a geometric stress concentrator $(Z \subseteq X)$, whose overall surface topology ∂Z is characterized by the following superposition of functions, describing its geometry at different scale levels:

$$f(x)=f_1(x)\circ f_2(x)\circ\ldots\circ f_n(x), \tag{3}$$

where $f_i(x)$ is a function with smoothness level 0 or higher, describing the surface geometry at the i-th scale level, $\circ$ denotes the superposition operator, $x \in \partial Z$.

For simplification of the problem of determining the influence of the concentrator geometry topology, this superposition is represented in the form of an n-dimensional vector:

$$N=\left(f_1(x),\ldots,f_n(x)\right). \tag{4}$$

Additionally, based on physical considerations, it is assumed that the functions are subject to the following constraints of the form:

$$Q_i^1(x)\le f_i(x)\le Q_i^2(x),\ x\in\partial Z. \tag{5}$$

A constraint of type (5) can be considered a simple specification of the upper or lower bound of the change of the function when considering the body as a Euclidean space, or in the form of a functional with a broader mathematical interpretation of the body region as a Hilbert space. In this case, limits of the quantities should be determined from the physical content of the problem.

As a result of external loading, fields of displacements, strains, and stresses are formed in the structural element, determined in accordance with model (2) and Hooke's law.

Since the parameters of the stress state do not uniquely determine the performance of structural elements, the following expression is used to analyze the strength of the body in a local region, which is defined as the pointwise strength of the structure:

$$k(x)=\frac{\sigma_0(x)-\sigma_*(x)}{\sigma_0(x)}, \tag{6}$$

where $k(x)$ is the safety factor, $\sigma_*(x)$ is the scalar equivalent of the stress tensor in the von Mises form, and $\sigma_0(x)$ is the scalar strength equivalent of the material.

An analysis of expression (6) shows that the functional $k(x)$ must satisfy the condition $0<k(x)\le 1$ for a material whose stress level is below the threshold at which material weakening occurs, i.e., when $k(x)\le 0$.

It is assumed that the optimal performance criterion for the structural element corresponds to the maximum average integral value of the expression $k(x)$:

$$L = \frac{1}{V}\int_V k(x)\,dx \to \max, \tag{7}$$

where V is the volume of the domain under consideration.

The advantage of an integral evaluation of the change in contact strength is that it is less sensitive to random value fluctuations, more realistically describes the loss of strength in the target volume, is resistant to reduced mesh quality, and accounts for material heterogeneity, local stochasticity, and anisotropy of the material. Normalization by the value V of the functional L was carried out to allow for the assessment of the dimensional factor of the structure and its strength parameters.

The functional (6) depends on the boundary conditions, the distribution of damage within the body, the material properties, and the surface topology of the stress concentrator:

$$L \equiv L\left(\partial X_1, \partial X_2, \partial X_3, \omega(x), K(x), G(x), \{f_1(x), \ldots, f_n(x)\}\right). \tag{8}$$

It should be noted that this problem formulation is general.

The focus is placed on the problem of varying the functional (8) with respect to the components of vector N, namely, the determination of such functions $f_1(x), \ldots, f_n(x)$ that maximize functional (8) subject to constraints (5).

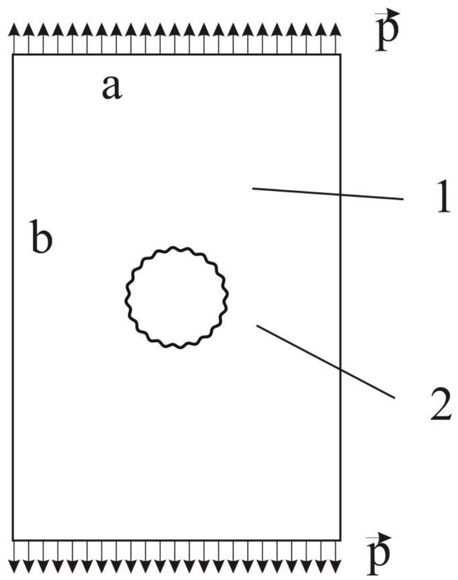

Fig. 1. Generalized problem formulation illustrating the object under study: 1 – rectangular body of dimensions a × b; 2 – stress concentrator of radius R with surface roughness; $\vec{p}$ – distributed load

To investigate the influence of the components of vector N (i.e., the superposition of functions $f_i(x)$, $i = 1...n$) on the distribution of strength parameters, a two--dimensional problem is formulated for a rectangular body subjected to mechanical loading and containing a circular stress concentrator of radius R at its center.

It is assumed that the surface of the circular stress concentrator is not perfectly smooth but is represented as a superposition of functions that also account for surface roughness (Fig. 1).

At present, surface roughness, which in engineering is understood as the set of surface micro-irregularities with relatively small spacing over a base length, is regulated by numerous international and national standards. In this study, the international standard ISO 4287 "Surface texture: Profile method – Terms, definitions and surface texture parameters" [17], as well as the scientific works [18, 19], were used.

The real surface of the body is modeled as a superposition of a base profile – a circle $f_1(x)$ – and a wave function $f_2(x)$:

$$f_1(x) = \left(R\cos(t), R\sin(t)\right), \tag{9}$$

$$f_2(x) = A\cos(kt)\overrightarrow{n(x)}, \tag{10}$$

$$\overrightarrow{n(x)} = \left(\cos(t), \sin(t)\right), \tag{11}$$

where R is the circle radius, A is the roughness amplitude, $t \in [0, 2\pi]$.

In equation (11), $\overrightarrow{n(x)}$ is the normal vector to the tangent curve $f_1(x)$ at point x.

As a result, the sought equation takes the following form:

$$f(x) = f_1(x) + f_2(x), \tag{12}$$

The following input data are used for numerical simulations: body dimensions $a = 100\cdot10^{-3}$ m, $b = 200\cdot10^{-3}$ m, radius of the circular stress concentrator $R = 20\cdot10^{-3}$ m, material properties (steel) – $K = 150\cdot10^9$ Pa (bulk modulus), $G = 80\cdot10^9$ Pa (shear modulus), $\sigma_0 = 650\cdot10^6$ Pa (ultimate strength), applied load along the lower and upper boundaries of the body is $\left|\vec{p}\right| = 10^8$ Pa. The surface roughness amplitude (parameter A in equation (10)) is varied from 0 m to $5\cdot10^{-6}$ m, which corresponds to the range of roughness values obtained in drilling processes (from $1.6\cdot10^{-6}$ m to $3.5\cdot10^{-6}$ m) [20]. The quantity A in this formulation of the problem has the dimension of linear length (micrometers or 10^{-6} m).

It is important to give an additional explanation for modeling a real body surface using an equation of type (12). Each mathematical model is based on certain a priori physical assumptions that must be justified. In this work, roughness is represented by one periodic function. This type of mathematical approximation of the surface can be used in the case when the surface is obtained by the same type of mechanical processing and it is necessary to take into account the main patterns of microrelief during modeling, rather than focusing on random surface fluctuations.

3. Solution procedure. Analysis of strength parameter distribution in bodies with surface stress concentrators

To obtain the solution of the continuum mechanics problem formulated in Section 2, a computational implementation of the finite element method using the open-source FEniCS package (Python-based) was employed. Graphical post-processing of the results was performed using the Matplotlib package [21].

The problem for model (2) was solved using the finite element method based on the method of weighted residuals, where the weighting function was chosen as the vector $\vec{v}$:

$$\int_{\Omega}\left(\vec{\nabla}\cdot\left(\frac{K(x)}{1-\omega(x)}\left(\vec{\nabla}\cdot\vec{u}\right)\hat{I}+\frac{2G(x)}{1-\omega(x)}\left(\vec{\nabla}\otimes\vec{u}-\frac{1}{3}\left(\vec{\nabla}\cdot\vec{u}\right)\hat{I}\right)\right)\right)\cdot\vec{v}dx=0, \quad (13)$$

where Ω is the integration domain, $\cdot$ denotes the scalar product, and $\vec{v}$ is the weighting function. The weight function has the same dimension as the desired quantity, but it is most often interpreted as a virtual (or imaginary) displacement.

Taking into account Hooke's law and applying integration by parts, the following equation is obtained:

$$\int_{\Omega}\left(\vec{\nabla}\cdot\hat{\sigma}\right)\cdot\vec{v}dx=-\int_{\Omega}\hat{\sigma}\cdot\cdot\left(\vec{\nabla}\otimes\vec{v}\right)dx+\int_{\partial\Omega}\left(\hat{\sigma}\cdot\vec{n}\right)\cdot\vec{v}ds, \quad (14)$$

Using the relation $\vec{T}=\hat{\sigma}\cdot\vec{n}$, where $\vec{T}$ is the surface traction vector, the following expression is obtained:

$$\begin{aligned}\int_{\Omega}\left(\vec{\nabla}\cdot\hat{\sigma}\right)\cdot\vec{v}dx&=-\int_{\Omega}\hat{\sigma}\cdot\cdot\left(\vec{\nabla}\otimes\vec{v}\right)dx+\int_{\partial\Omega}\vec{T}\cdot\vec{v}ds=\\&=-\int_{\Omega}\hat{\sigma}\cdot\cdot\left(\vec{\nabla}\otimes\vec{v}\right)dx+\int_{\partial\Omega_1}\vec{T}\cdot\vec{v}ds+\int_{\partial\Omega_2}\vec{T}\cdot\vec{v}ds,\end{aligned} \quad (15)$$

where $\partial\Omega_1$, $\partial\Omega_2$ – lower and upper boundaries of the body.

The scalar equivalent of the stress tensor in the von Mises form is given by:

$$\hat{\sigma}_0=\sqrt{\frac{3}{2}\hat{s}\cdot\cdot\hat{s}}, \quad (16)$$

where $\hat{s}=\hat{\sigma}-\frac{1}{3}tr(\hat{\sigma})\hat{I}$, $tr(\hat{\sigma})=\left(\hat{\sigma}\cdot\cdot\hat{I}\right)^2$.

For numerical experiments using the finite element method, the object under study was discretized using a non-uniform mesh with additional refinement in the stress concentrator region.

To increase the accuracy of the solution, this article uses a second-order CG (Continuous Galerkin) finite element. As a result, instead of three nodal points (as in a conventional linear finite-element decomposition), six nodal points are formed on each mesh cell (in this case, a triangle), and the basis functions become quadratic. This allows us to approximate both the desired quantity and its gradient with sufficient accuracy.

The numerical simulations were performed on a computer with the following specifications: Intel i7-3630QM ×8 CPU, 8 GB RAM, operating system Ubuntu 23.10.

The average size of the base finite element was 0.16 mm, while in the refined mesh region it was 0.0003 mm. The total number of finite elements was 133,817. This mesh size was chosen to increase the accuracy of the solution of the problem. At the same time, such a small size of the finite element leads to the appearance of certain mathematical limitations that require their physical justification. The average size of the compacted grid is 0.003 mm, which is smaller than the average size of grains in metals. Each grain within its region has the property of anisotropy, but since the calculation is performed on a significant number of points falling on different grains, which are generally not oriented in any particular direction, this discrete scheme preserves the property of isotropy. The average computation time per simulation was approximately 15 seconds.

The geometry of the object under study is shown in Figure 2.

a) b)

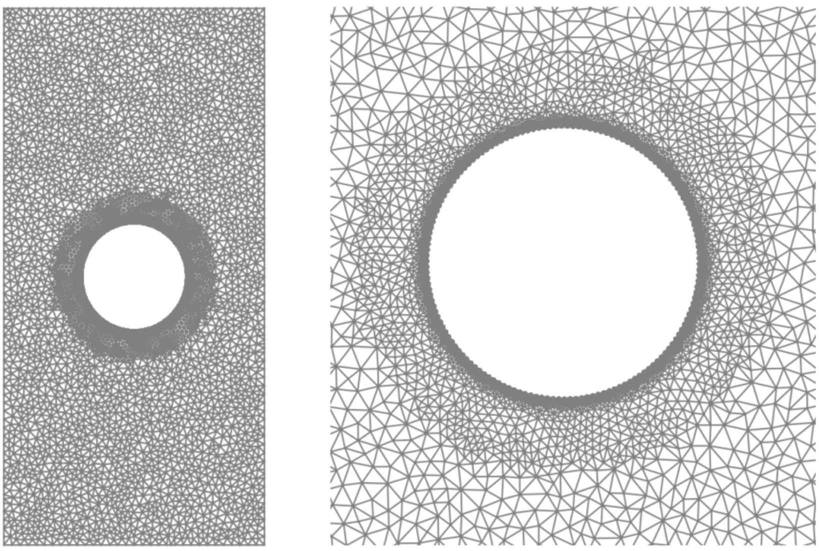

Fig. 2. General (a) and detailed (b) views of the object under study

The simulations performed showed that the presence of surface roughness on the stress concentrator alters the stress-strain state in the vicinity of the physical concentrator (Fig. 3).

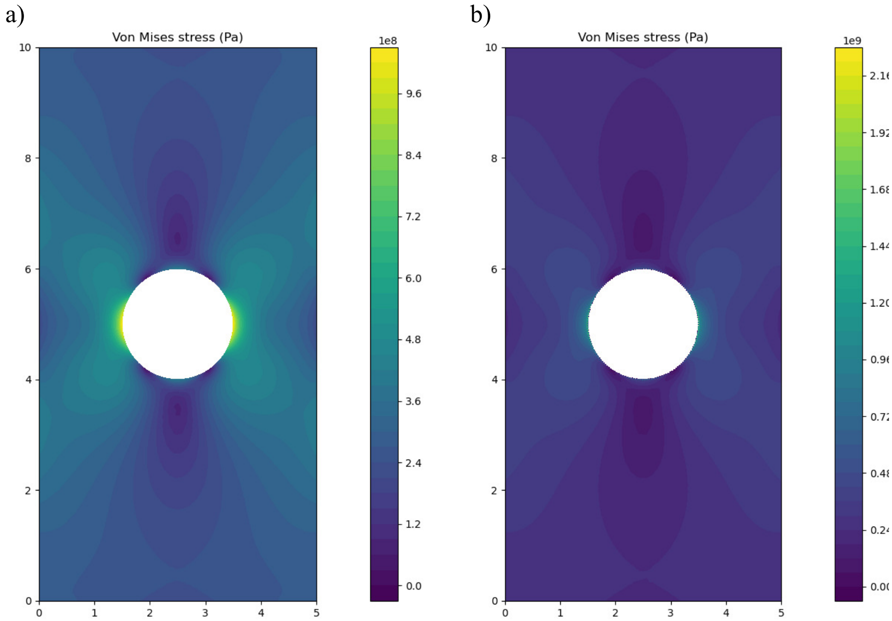

Fig. 3. Stress distribution in von Mises form in the absence (a) and presence (b) of surface roughness

Analysis of the obtained results indicates that surface roughness of the stress concentrator leads to an increase in stress levels. Such geometric irregularities act as sources of secondary stress perturbations, affecting the performance and reliability of components. For structures with circular stress concentrators without roughness, the maximum stress level is $1.03 \cdot 10^8$ Pa, whereas in the presence of surface roughness of $3.5 \cdot 10^{-6}$ m, it increases to $3.7 \cdot 10^8$ Pa.

Since the finite element approximation of objects with complex geometry can be sensitive to the parameters of their meshing, studies were conducted on the effect of mesh density on the values of maximum stresses. Three more sparse meshings of the object of study were considered, which is shown in Figure 1. These partitions are called Mesh 1, Mesh 2, and Mesh 3. Mesh 1 has the following parameters: the average size of the main finite element is 0.2 mm, for the compacted mesh – 0.004 mm, the number of finite elements – 122008. Mesh 2 has the following parameters: the average size of the main finite element is 0.26 mm, for the compacted mesh – 0.006 mm, the number of finite elements – 105006. Mesh 3 has the following parameters: the average size of the main finite element is 0.3 mm, for the compacted mesh – 0.008 mm, the number of finite elements – 65513. The initial mesh partition was called mesh 0.

The results of the calculations are summarized in Table 1.

Table 1. Dependence of the maximum stress value on the mesh parameters

Mesh type	Maximum stress level, 10^8 Pa	
	for a stress concentrator without roughness	for stress concentrator with $3.5 \cdot 10^{-6}$ m roughness
Mesh 0	1.03	3.7
Mesh 1	1.03	3.7
Mesh 2	1.03	3.8
Mesh 3	1.03	3.6

As it can be seen from the research results, the values of maximum stresses are not very sensitive to the parameters of the grid division. This can be explained by the fact that nonlinear basis functions of the 2nd order were used for the calculations.

An analysis of the variation of parameter L (the integral strength measure) with respect to surface roughness was also performed (Fig. 4).

The roughness amplitude was varied from 0 to $5 \cdot 10^{-6}$ m with a step size of $0.05 \cdot 10^{-6}$ m (a total of 100 numerical experiments were conducted). The results are presented in Figure 5.

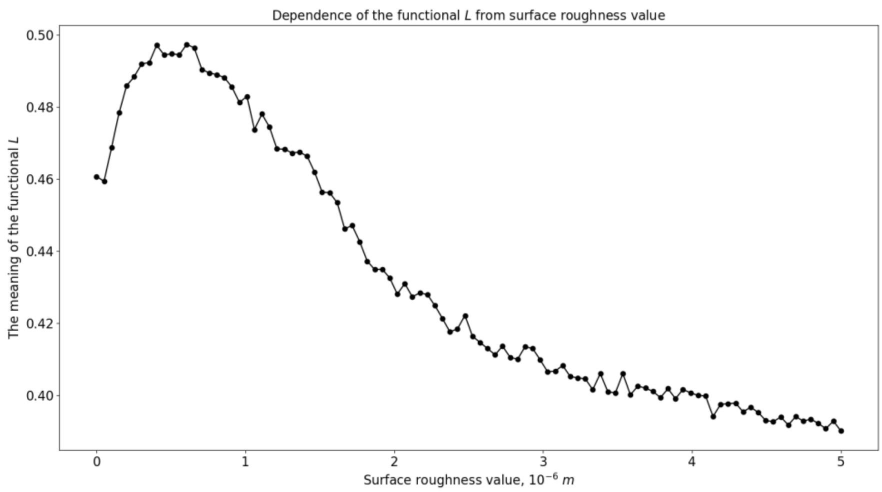

Fig. 4. Dependence of functional L on surface roughness

The analysis showed that for this type of circular stress concentrator, there exists an optimal roughness value in the range of $0.7\text{-}0.8 \cdot 10^{-6}$ m, at which the functional L (integral structural strength) increases.

The variation of the maximum stress level with respect to surface roughness was also analyzed (Fig. 5).

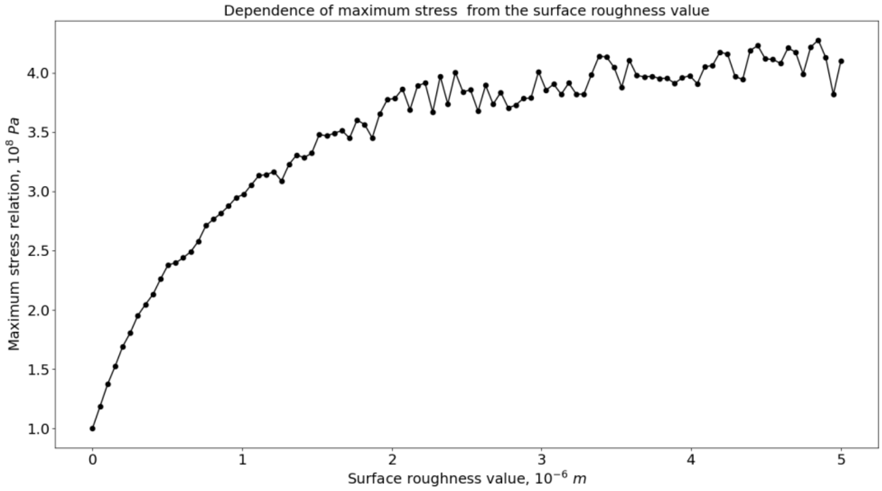

Fig. 5. Dependence of the maximum stress level on surface roughness

The study shows that when surface roughness exceeds $1.0 \cdot 10^{-6}$ m, the strength of the body under study decreases significantly, both due to material weakening and due to the increase in maximum stress levels.

At the same time, despite the increase in the maximum stress level with increasing roughness, at roughness values of approximately $0.7\text{-}0.8 \cdot 10^{-6}$ m, the overall strength of the component increases (Fig. 4). According to the classical Mechanics of Materials' theory, the degree of smoothness of the surface of the stress concentrator is directly correlated with the level of maximum stresses. This is also shown in Figure 5. Therefore, the results obtained in the work, shown in Figure 4, at first glance may be in some contradiction with engineering models of mechanics. Without denying these results, it is noted that the presence of technologically formed roughness on the surface of the concentrator, the peaks and valleys of which also act as sources of additional stress disturbances, leads to "smearing" of the initial stress-strain state of the body due to the redistribution of stresses, which can also lead to an increase in the operational strength of products. The results obtained are in good agreement with the modern concept of controlling the stress intensity coefficient in parts using the geometric characteristics of surface roughness [22].

This leads to an important practical conclusion: to improve the performance of components containing internal stress concentrators, it is necessary to ensure an optimal level of roughness of the internal surfaces. For a circular stress concentrator with the given geometric parameters, this optimal roughness is approximately $0.75 \cdot 10^{-6}$ m. It should be additionally noted that the established numerical values of the optimal surface roughness parameters are characteristic of this product (a circular type of stress concentrator) under a given type of force loads.

4. Conclusions

1. The article considers a numerical study of the problem of the influence of the regular geometric microrelief of the internal surfaces of stress concentrators on the strength parameters of products.
2. It has been shown that the internal surface roughness of stress concentrators significantly alters the stress-strain state of the component, rendering it non-uniform. Moreover, surface valleys act as sources of additional stress perturbations, substantially distorting the initial stress distribution.
3. An increase in surface roughness leads to higher maximum stresses in the components. Therefore, it is necessary to implement technological solutions that ensure an optimal level of internal surface roughness during manufacturing. For steel with the above mechanical properties, this optimal roughness lies in the range of $0.7\text{-}0.8 \cdot 10^{-6}$ m.

References

[1] Gross, D., & Seelig, T. (2011). *Fracture Mechanics with an Introduction to Micromechanics*. Springer. DOI: 10.1007/978-3-642-19240-1.

[2] Sivak, P., Delyova, I., & Bocko, J. (2023). Comparison of stress concentration factors obtained by different methods. *Applied Sciences*, *13*(24), 13328. DOI: 10.3390/app132413328.

[3] Pilkey, W.D., Pilkey, D.F., & Bi, Z. (2020). *Peterson's Stress Concentration Factors* (4th ed.). Wiley.

[4] Murakami, Y. (2017). *Theory of Elasticity and Stress Concentration*. John Wiley & Sons.

[5] Savruk, M., & Kazberuk, A. (2017). *Stress Concentration at Notches*. Springer. DOI: 10.1007/978-3-319-44555-7.

[6] Pramanik, A., Dixit, A.R., Chattopadhyaya, S., Uddin, M.S., Dong, Yu., Basak, A.K., & Littlefair, G. (2017). Fatigue life of machine components. *Advances in Manufacturing*, *5*, 59-76. DOI: 10.1007/s40436-016-0168-z.

[7] Blais, P., Toubal, L., & Zitoune, R. (2024). The influence of the hole-generation process on fatigue response of open-hole and assembled titanium samples. *Journal of Manufacturing Processes*, *110*, 412-423. DOI: 10.1016/j.jmapro.2024.01.007.

[8] Lipiäinen, K., Afkhami, S., Ahola, A., & Ahola, T. (2022). Evaluation of geometrical notch and quality effects in the fatigue strength assessment of ultra-high-strength steel cut edges. *Structures*, *37*, 881-892. DOI: 10.1016/j.istruc.2022.01.069.

[9] Dahlan, H., Rusli, M., & Bur, M. (2018). The reduction of the stress concentration of the crack tip using multi stop-drilled hole. *Journal of Ocean, Mechanical and Aerospace – Science and Engineering (JOMAse)*, *55*(1), 6-10. DOI: 10.36842/jomase.v55i1.54.

[10] Macoretta, G., Monelli, B.D., Arcioni, M., & Grilli, M. (2024). Effects of deep drilling processes on the fatigue strength of GTD-111 DS. *International Journal of Fatigue*, *188*, 108525. DOI: 10.1016/j.ijfatigue.2024.108525.

[11] Zhang, Y., Zhou, M., Gao, W., Liu, X., & Peng, Z. (2026). Trajectory method versus forming method – influence of turning-indicated surface integrity on fatigue performance of V-shaped notch specimens. *Measurement*, *270*, 120724. DOI: 10.1016/j.measurement.2026.120724.

[12] Feng, W., Liu, H., Fan, T., Tang, Y., & Zhang, J. (2025). Effects of cutting speed on surface integrity evolution and fatigue behavior of shot-peened Inconel 718 in sequential turning and shot peening. *Engineering Failure Analysis*, *179*, 109817. DOI: 10.1016/j.engfailanal.2025.109817.

[13] Kopylov, V., Kuzin, O., & Kuzin, N. (2019). Improving contact durability of polycrystalline systems by controlling the parameters of long-angle grain boundaries. *Eastern-European Journal of Enterprise Technologies*, *5*(12(101)), 14-22. DOI: 10.15587/1729-4061.2019.181441.

[14] Oreavbiere, A., & Khan, M. (2024). Mathematical complexities in modelling damage in spur gears. *Machines*, *12*(5), 346. DOI: 10.3390/machines12050346.

[15] Luchko, Y.Y., Kuzin, O.A., Kopylov, V.I., & Kuzin, M.O. (2023). Assessment approaches to optimum surface hardening parameters of stress concentrator-bearing structures. *Strength of Materials*, *55*(4), 720-726. DOI: 10.1007/s11223-023-00561-0.

[16] Kuzin, N.O. (2015). A mathematical model describing the variation in material properties. *International Applied Mechanics*, *51*(4), 471-479. DOI: 10.1007/s10778-015-0708-4.

[17] International Organization for Standardization (1997). *Geometrical product specifications (GPS) – Surface texture: Profile method – Terms, definitions and surface texture parameters* (ISO 4287:1997).

[18] Yuechang, W., Ying L., & Hongju L. (2022). A review of rough surface simulation methods. *Journal of Mechanical Engineering*, *58*(19), 148-165. DOI: 10.3901/JME.2022.19.148.

[19] Borodich, F.M., Pepelyshev, A., & Jin, X. (2024). A multiscale statistical analysis of rough surfaces and applications to tribology. *Mathematics*, *12*, 1804. DOI: 10.3390/math12121804.

[20] Jeyamohan, R., Dhayanithi, S., Krishnaswamy, H., Astarita, A., & Narayanan A. (2024). A comprehensive investigation on the effect of processing conditions on the dry drilling performance of electron beam melting-manufactured Ti6Al4V. *The International Journal of Advanced Manufacturing Technology*, *132*(5-6), 2427-2441. DOI: 10.1007/s00170-024-13504-z.

[21] Johansson, R. (2019). *Numerical Python: Scientific Computing and Data Science Applications with Numpy, SciPy and Matplotlib*. Apress. DOI: 10.1007/978-1-4842-4246-9.

[22] Zhao, B., Song, J., Xie L., Hu, Z., & Chen, J. (2021). Surface roughness effect on fatigue strength of aluminum alloy using revised stress field intensity approach. *Scientific Reports*, *11*(1), 19279. DOI: 10.1038/s41598-021-98858-0.